# Theory of the Aharonov-Bohm effect in carbon nanotubes

**Tsuneya Ando**

Department of Physics, Tokyo Institute of Technology,
2-12-1 Ookayama, Meguro-ku, Tokyo 152-8551, Japan

**Abstract.** A brief review is given on electronic properties of carbon nanotubes with emphasis on Aharonov-Bohm effects on the band structure. The topics include an effective-mass description of electronic states, magnetic properties, optical absorption, and transport.

## 1. Introduction

Carbon nanotubes (CN) are either a metal or semiconductor, depending on their diameters and helical arrangement. This condition can be obtained based on the band structure of a two-dimensional (2D) graphite sheet and periodic boundary conditions along the circumference direction. This result was predicted by means of a tight-binding model and also by a $\mathbf{k}\cdot\mathbf{p}$ method or an effective-mass approximation [1]. The cylindrical shape leads to a strong Aharonov–Bohm (AB) effect in the band structure due to a magnetic field parallel to the axis [2, 3]. The purpose of this paper is to give a brief review of the AB effect on electronic and transport properties of carbon nanotubes, predicted in the $\mathbf{k}\cdot\mathbf{p}$ scheme.

## 2. Effective-mass description

A graphite sheet is a zero-gap semiconductor in the sense that the conduction and valence bands consisting of $\pi$ states cross at K and K' points of the Brillouin zone [4]. The structure is shown in Fig. 1 together with the first Brillouin zone and coordinate systems to be used in the following. Electronic states near a K point are described by the $\mathbf{k}\cdot\mathbf{p}$ equation [1, 5]:

$$\gamma(\vec{\sigma}\cdot\hat{\mathbf{k}})\mathbf{F}(\mathbf{r})=\varepsilon\mathbf{F}(\mathbf{r}),\quad \mathbf{F}(\mathbf{r})=\begin{pmatrix}F_A(\mathbf{r})\\F_B(\mathbf{r})\end{pmatrix}, \tag{1}$$

where $\gamma$ is the band parameter, $\hat{\mathbf{k}}=(\hat{k}_x,\hat{k}_y)=-i\vec{\nabla}$ is a wave-vector operator, $\varepsilon$ is the energy, and $\sigma_x$ and $\sigma_y$ are the Pauli spin matrices. Two components of the wave function $\mathbf{F}(\mathbf{r})$ correspond to the amplitude at A and B sites in a unit cell. Equation (1) has the form of Weyl's equation for neutrinos.

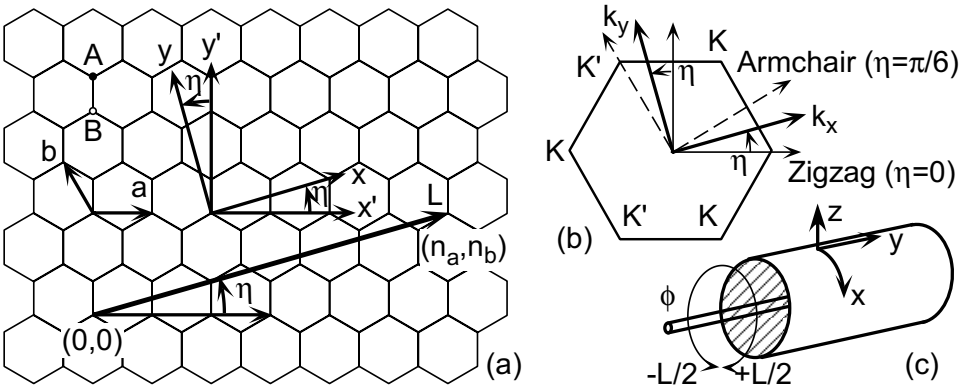


**Figure 1.** (a) Lattice structure of a two-dimensional graphite sheet. The coordinates $(x',y')$ are fixed on the graphite sheet and $(x,y)$ are chosen in such a way that $x$ is along the circumference and $y$ is along the axis. $\eta$ is the chiral angle. (b) The first Brillouin zone and K and K' points. (c) The coordinates for the nanotube. An Aharonov-Bohm flux $\phi$ is applied in the axis direction of the nanotube.

An important feature of the Weyl equation is the presence of a topological singularity at $\mathbf{k}=0$. A neutrino has a helicity and its spin is quantized into the direction of its motion. The spin eigen function changes its signature due to Berry's phase under a $2\pi$ rotation. Correspondingly, the wave function acquires phase $-\pi$ when $\mathbf{k}$ is rotated around the origin along a closed contour [6, 7]. The signature change occurs only when the closed contour encircles the origin $\mathbf{k}=0$ but not when the contour does not contain $\mathbf{k}=0$. This topological anomaly leads to the absence of backward scattering and the perfect conductance even in the presence of scatterers unless their potential range is smaller than the lattice constant of 2D graphite [8].

A singularity at $\varepsilon=0$ manifests itself in a magnetic field $B$. Semiclassically, the Landau levels can be obtained as $\varepsilon_n=\sqrt{|n|+\delta}\,\mathrm{sgn}(n)(\sqrt{2}\gamma/l)$ with integer $n$ and an appropriate small correction $\delta$, where $l$ is the magnetic length given by $\sqrt{c\hbar/eB}$ and $\mathrm{sgn}(t)$ stands for the signature of $t$. There can be no Landau level at $\varepsilon=0$. However, a full quantum mechanical treatment gives $\varepsilon_n=\sqrt{|n|}\,\mathrm{sgn}(n)\,(\sqrt{2}\gamma/l)$, leading to the formation of Landau levels at $\varepsilon=0$.

The structure of a nanotube is specified by a chiral vector $\mathbf{L}$ corresponding to the circumference. In the following we shall choose the $x$ axis in the circumference direction and the $y$ axis in the axis direction, i.e., $\mathbf{L}=(L,0)$ with $L=|\mathbf{L}|$. The angle $\eta$ between $\mathbf{L}$ and the horizontal axis is called the chiral angle.

The electronic states can be obtained by imposing the periodic boundary condition in the circumference direction $\psi(\mathbf{r}+\mathbf{L})=\psi(\mathbf{r})$ except in extremely thin CNs. The Bloch functions at a K point change their phase by $\exp(i\mathbf{K}\cdot\mathbf{L})=\exp(2\pi i\nu/3)$, where $\nu=0$ or $\pm1$, determined by $\mathbf{L}$. Because $\psi(\mathbf{r})$ is written as a product of the Bloch function and the envelope function, this phase change should be canceled by that of the envelope functions and the boundary conditions for the envelope functions are given by $\mathbf{F}(\mathbf{r}+\mathbf{L})=\mathbf{F}(\mathbf{r})\exp(-2\pi i\nu/3)$.

A nonzero curvature causes a shift in the origin of $\hat{k}_x$ and $\hat{k}_y$ in the $\mathbf{k}\cdot\mathbf{p}$ Hamiltonian. The shift in the $y$ direction is irrelevant and that in the $x$ direction can be replaced by an effective flux $\phi_c$. The flux was estimated as [9, 10]

$$\frac{\phi_c}{\phi_0}=\frac{2\pi}{4\sqrt{3}}\frac{a}{L}p\cos 3\eta, \tag{2}$$

with $\phi_0=ch/e$ being the flux quantum, $a$ the lattice constant of the two-dimensional graphite,

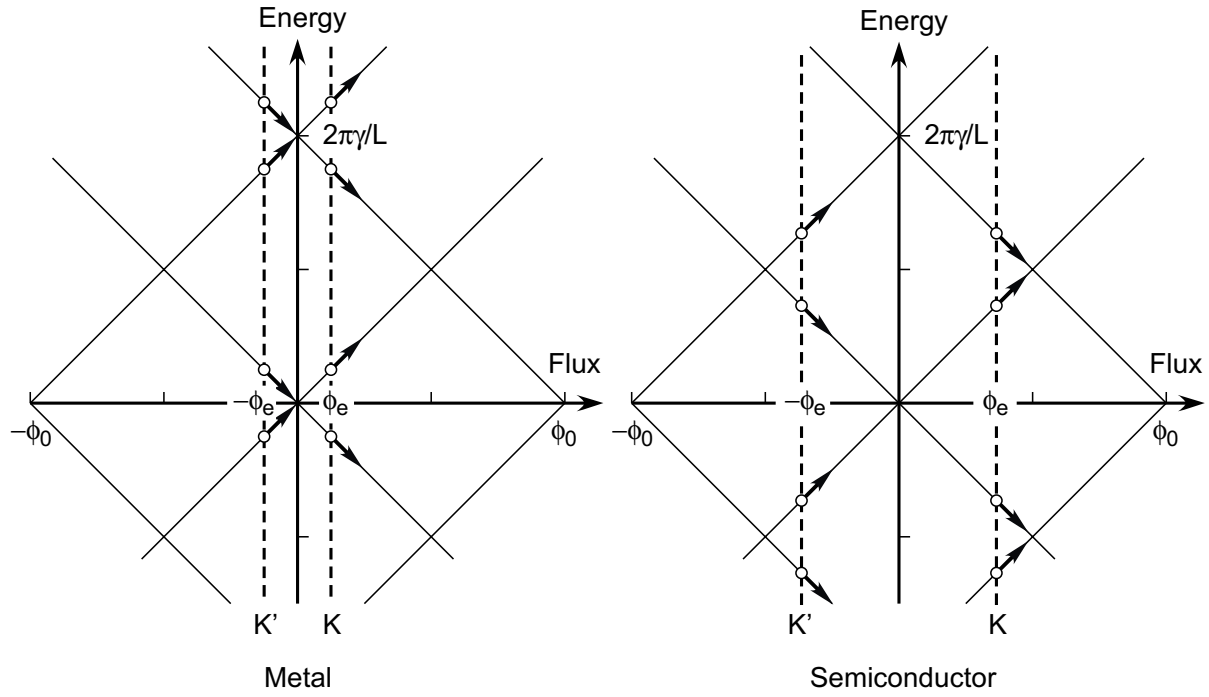


**Figure 2.** The band edges $\pm(2\pi\gamma/L)|n+(\phi/\phi_0)|$ as a function of $\phi$. In the presence of an effective flux $\phi_e$ due to curvature and/or strain, we have $\phi=\phi_e$ for the K point and $\phi=-\phi_e$ for the K' point. An AB magnetic flux shifts $\phi$ in the positive direction as shown by arrows.

$p=1-(3/8)\gamma'/\gamma$, $\gamma=-(\sqrt{3}/2)V_{pp}^{\pi}a$, and $\gamma'=-(\sqrt{3}/2)(V_{pp}^{\sigma}-V_{pp}^{\pi})a$, where $V_{pp}^{\pi}$ $(=-\gamma_0)$ and $V_{pp}^{\sigma}$ are the conventional tight-binding parameters for neighboring $p$ orbitals [10]. The curvature effect is largest in zigzag nanotubes with $\eta=0$ and absent in armchair nanotubes with $\eta=\pi/6$.

The presence of a lattice distortion $\mathbf{u}=(u_x,u_y,u_z)$ causes also an effective flux. It is estimated as [11]

$$\frac{\phi_s}{\phi_0}=\frac{Lg_2}{2\pi\gamma}[(u_{xx}-u_{yy})\cos 3\eta-2u_{xy}\sin 3\eta], \tag{3}$$

where $u_{\mu\nu}$ $(\mu,\nu=x,y)$ denotes the lattice strain given by

$$u_{xx}=\frac{\partial u_x}{\partial x}+\frac{2\pi u_z}{L},\quad u_{yy}=\frac{\partial u_y}{\partial y},\quad 2u_{xy}=\frac{\partial u_x}{\partial y}+\frac{\partial u_y}{\partial x}, \tag{4}$$

and $g_2$ is the electron-phonon interaction energy given by $g_2=(\alpha/2)\gamma_0$ with $\alpha\sim 1$, where $\gamma=\sqrt{3}a\gamma_0/2$ [11, 12]. This shows that twist and stretch deformation give rise to nonzero flux in armchair and zigzag nanotubes, respectively.

In summary, electronic states in nanotubes can be specified by a single parameter $\varphi_e$ defined by

$$\varphi_e=-\frac{\nu}{3}+\varphi_c+\varphi_s,\qquad \varphi_c=\frac{\phi_c}{\phi_0},\qquad \varphi_s=\frac{\phi_s}{\phi_0}, \tag{5}$$

and energy levels for the K point are obtained by putting $k_x=\kappa_{\varphi_e}(n)$ with $\kappa_{\varphi_e}(n)=(2\pi/L)(n+\varphi_e)$ and $k_y=k$ in the above $\mathbf{k}\cdot\mathbf{p}$ equation as $\varepsilon_{\varphi_e}^{(\pm)}(n,k)=\pm\gamma\sqrt{\kappa_{\varphi_e}(n)^2+k^2}$, where $n$ is an integer and the upper $(+)$ and lower $(-)$ signs represent the conduction and valence bands,

respectively. For the K' point, the Schrödinger equation is given by replacing $\hat{k}_y$ with $-\hat{k}_y$ and the boundary condition gives an effective flux $-\varphi_e$ leading to $k_x = \kappa_{-\varphi_e}(n)$. When $\phi_c = \phi_s = 0$, a nanotube becomes metallic for $\nu = 0$ and semiconducting with gap $\varepsilon_G = 4\pi\gamma/3L$ for $\nu = \pm 1$.

When a magnetic field is applied parallel to the axis, i.e., in the presence of a magnetic flux $\phi$ passing through the cross section, the AB flux leads to the change in the boundary condition $\psi(\mathbf{r}+\mathbf{L}) = \psi(\mathbf{r})\exp(+2\pi i\varphi)$, where $\varphi = \phi/\phi_0$. Consequently, $\kappa_{\varphi_e}(n)$ is replaced with $\kappa_{\varphi+\varphi_e}(n)$ for the K point and $\kappa_{-\varphi_e}(n)$ with $\kappa_{\varphi-\varphi_e}(n)$ for the K' point. The energy bands are given by $\varepsilon^{(\pm)}_{\varphi+\varphi_e}(n,k)$ and $\varepsilon^{(\pm)}_{\varphi-\varphi_e}(n,k)$ for the K and K' point, respectively. Figure 2 shows a schematic illustration of the band edges $\varepsilon^{(\pm)}_{\varphi\pm\varphi_e}(n,0)$. The gap exhibits an oscillation between 0 and $2\pi\gamma/L$ with period $\phi_0$ with the change in the AB flux $\phi$ [1]. This giant AB effect on the band gap is a unique property of nanotubes. The AB effect on the gap should appear in a tunneling conductance across a finite-length CN [13].

## 3. Magnetic properties

In the presence of AB flux, the magnetization is written as [2, 14]

$$M^{\parallel}(\varphi) = 2\mu_{\rm B}\frac{A}{a}\frac{2ma\gamma}{\hbar^2}[W(\varphi+\varphi_e)+W(\varphi-\varphi_e)], \tag{6}$$

where $\mu_B = e\hbar/2mc$ is the Bohr magneton and $W_1(\varphi)$ is a dimensionless quantity given analytically by

$$W(\varphi) = -\frac{1}{2\pi}\int_0^{\varphi}\ln(2\sin\pi t)\,dt, \tag{7}$$

for $0 < \varphi < 1$ [9, 15]. The value of $W(\varphi)$ outside this region is obtained by using $W(\varphi+j) = W(\varphi)$ with integer $j$. In the vicinity of $\varphi = j$, $W \approx -(2\pi)^{-1}(\varphi-j)\ln|\varphi-j|$. Therefore, the moment itself vanishes but its derivative diverges logarithmically (positive infinite) at $\varphi = j$ and metallic CN's exhibit paramagnetism in a weak parallel field in the absence of $\phi_c$ and $\phi_s$. On the other hand, semiconducting nanotubes exhibit a weak diamagnetism.

In the presence of a weak magnetic field perpendicular to the tube axis, the nanotube exhibits large diamagnetism corresponding to the anomaly at $\varepsilon = 0$ mentioned in the previous section. The susceptibility is only a weak function of $\varphi$ (and $\varphi_e$) and the average over $\varphi$ is given by

$$\bar{\chi}^{\perp} = -\frac{\gamma L}{16\pi}\left(\frac{e}{c\hbar}\right)^2. \tag{8}$$

The susceptibility is proportional to the circumference $L$ and therefore diverges in the limit of infinitely large $L$. This dependence is closely related to the susceptibility of a 2D graphite sheet $\chi = -(\gamma^2/3\pi\mu)(e/c\hbar)^2$ with the Fermi energy $\mu$ [16], which diverges for $\mu = 0$. The above susceptibility can be obtained by replacing $\mu$ with $(8/3\pi)(2\pi\gamma/L)$, which is of the order of the typical confining energy due to a finite circumference. Nanotubes have a strong tendency to align in the direction of a magnetic field, because of the large diamagnetic susceptibility, independent of whether they are semiconducting or metallic.

## 4. Aharonov-Bohm effect on optical transition

The interband optical absorption corresponding to the states in the vicinity of the K and K' points can be observed only for the light polarization parallel to the CN axis [17]. Further,

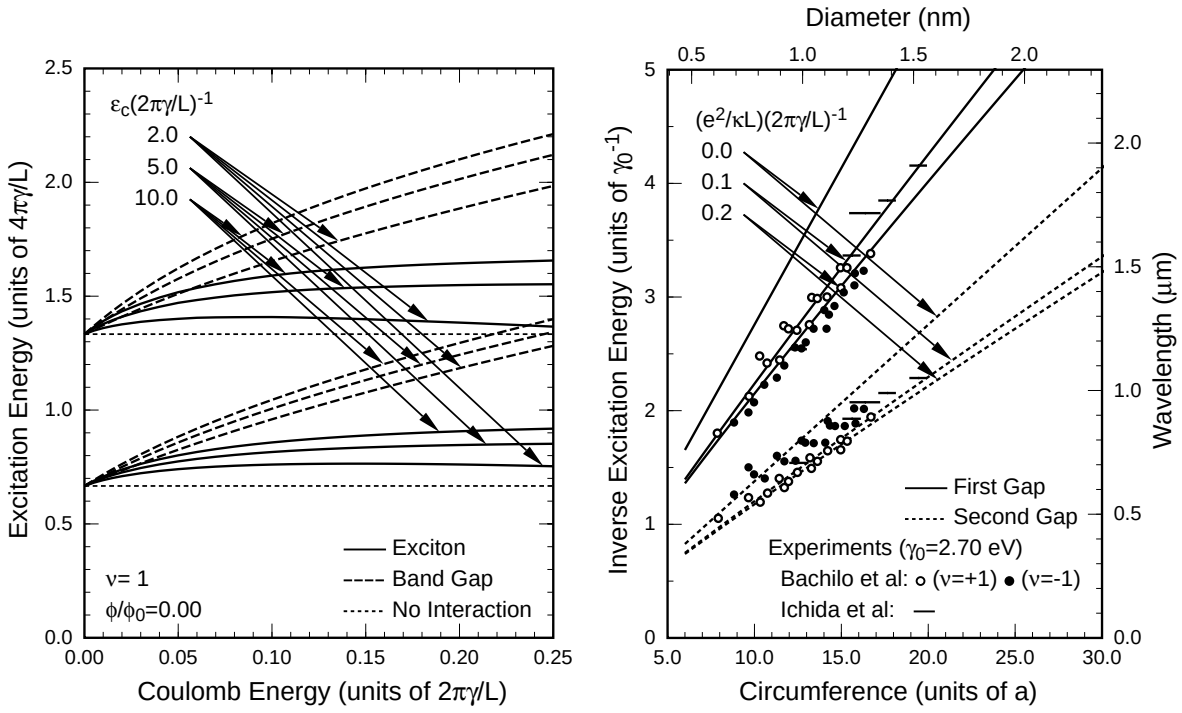


**Figure 3.** (a) Calculated excitation energies as a function of the effective Coulomb energy $(e^2/\kappa L)/(2\pi\gamma/L)$ in a semiconducting nanotube with $\phi_c = \phi_s = \phi = 0$. (b) The inverse of the absorption energies as a function of the circumference and the diameter. The experimental results (Ichida et al. [21, 22] and Bachilo et al. [23]) are plotted using $\gamma_0 = 2\gamma/\sqrt{3}a = 2.7$ eV.

for the parallel polarization transitions are allowed only between bands with same $n$ [17]. The corresponding band gap is given by $\varepsilon_G^K(n) = 2\gamma|\kappa_{\varphi+\varphi_e}(n)|$ for the K point and by $\varepsilon_G^{K'}(n) = 2\gamma|\kappa_{\varphi-\varphi_e}(n)|$ for the K' point, respectively.

Consider a semiconducting nanotube with $\nu = 1$, for example. For a small magnetic flux $\varphi \ll 1$, the lowest conduction band and the highest valence band are given by $n = 0$ for both K and K' points. At the K point, $\kappa_{\varphi+\varphi_e}(0) = -(2\pi/L)[(1/3) - \varphi_c - \varphi_e - \varphi]$ and the corresponding band gap is given by $\varepsilon_G^K(0) = (2/3)(2\pi\gamma/L)(1 - 3\varphi_c - 3\varphi_s - 3\varphi)$. At the K' point, on the other hand, $\kappa_{\varphi-\varphi_e}(0) = (2\pi/L)[(1/3) - \varphi_c - \varphi_s + \varphi]$ and the corresponding band gap is given by $\varepsilon_G^{K'}(0) = (2/3)(2\pi\gamma/L)(1 - 3\varphi_c - 3\varphi_s + 3\varphi)$. Therefore, the band gaps of the K and K' points split in the presence of $\varphi$. The splitting is proportional to the flux, i.e., $\varepsilon_G^K(0) - \varepsilon_G^{K'}(0) = -4(2\pi\gamma/L)\varphi$.

The second conduction and valence bands are given by $n = +1$ for the K point and $n = -1$ for the K' point in the case $\nu = 1$. The corresponding band gaps are given by $\varepsilon_G^K(+1) = (2/3)(2\pi\gamma/L)(2 + 3\varphi_c + 3\varphi_s + 3\varphi)$ and $\varepsilon_G^{K'}(-1) = (2/3)(2\pi\gamma/L)(2 - 3\varphi_c - 3\varphi_s - 3\varphi)$. The amount of the splitting is same as that of the lowest gap, but the direction is different. The results for $\nu = -1$ can be obtained by exchanging K and K' points. Note that the band gap is shifted by the effective flux due to curvature and strain, but no splitting appears between K and K' points.

We have to take into account effects of electron-electron interaction on the band structure and excitonic interaction between an electron and a hole excited optically [18]. The strength of the Coulomb interaction is specified by $(e^2/\kappa L)/(2\pi\gamma/L)$. This parameter is independent

of $L$ and estimated as $(e^2/\kappa L)(L/2\pi\gamma) = 0.35/\kappa$. The static dielectric constant $\kappa$ describes polarization of states other than those lying in the vicinity of the Fermi level ($\pi$ and $\sigma$ bands and core level) and of surrounding materials. In bulk graphite we have $\kappa \approx 2.4$ [19] giving $(e^2/\kappa L)(L/2\pi\gamma) \sim 0.15$, but this simple constant screening is only a rough approximation. The interaction parameter is independent of the diameter and therefore the band gap and also the exciton binding energy are inversely proportional to $L$.

Explicit calculations of the band structure in the random-phase approximation shows that the energy gaps have a weak logarithmic dependence on $L$ due to the necessity of introducing a cutoff energy $\varepsilon_c$ corresponding to the $\pi$-band width, $\varepsilon_c(2\pi\gamma/L)^{-1} \sim (\sqrt{3}/\pi)(L/a)$ [12, 20]. Figure 3(a) shows band gaps and corresponding exciton energies as a function of $(e^2/\kappa L)/(2\pi\gamma/L)$ [12]. The band gaps are strongly enhanced but excitonic effects tend to cancel a large part of the enhancement. The same calculation of the band-edge effective-mass reveals that the interaction effect is weak. This means that the interaction effect cannot be expressed as a renormalization of the band parameter $\gamma$. The comparison with some of available experiments [21, 22, 23] shown in Fig. 3(b) shows the calculations explain essential features of the observed dependence on $L$.

This splitting of peaks in the presence of AB magnetic flux was recently observed in optical absorption and emission spectra [24]. The magnetic alignment of the nanotubes was observed also and used for the determination of the anisotropic magnetic susceptibility discussed in the previous section [25]. Explicit calculations of the band gaps and the exciton energies in the presence of AB magnetic flux shows that the amount of the splitting is not so strongly affected by the interaction [12].

In thin nanotubes, the trigonal warping of the bands should be considered. The warping can be incorporated by the inclusion of a higher order $\mathbf{k}\cdot\mathbf{p}$ term [26]. For the K point, for example, the Hamiltonian becomes

$$\mathscr{H} = \gamma \begin{pmatrix} 0 & \hat{k}_x - i\hat{k}_y + \dfrac{\beta a}{4\sqrt{3}} e^{3i\eta} (\hat{k}_x + i\hat{k}_y)^2 \\ \hat{k}_x + i\hat{k}_y + \dfrac{\beta a}{4\sqrt{3}} e^{-3i\eta} (\hat{k}_x - i\hat{k}_y)^2 & 0 \end{pmatrix}, \tag{9}$$

with $\beta$ being a dimensionless constant of the order of unity ($\beta = 1$ in a nearest-neighbor tight-binding model). This Hamiltonian gives the energy bands

$$\begin{aligned} \varepsilon^{(\pm)}_{\varphi+\varphi_e}(n,k) \approx \pm\gamma \Big[ \kappa_{\varphi+\varphi_e}(n)^2 \Big( 1 + \frac{\beta a \kappa_{\varphi+\varphi_e}(n)}{2\sqrt{3}} \cos 3\eta \Big) \\ + \Big( 1 - \frac{\sqrt{3}\beta a \kappa_{\varphi+\varphi_e}(n)}{2} \cos 3\eta \Big) (k - \Delta k)^2 \Big]^{1/2}, \end{aligned} \tag{10}$$

with $\Delta k = (\sqrt{3}\beta a/4)\kappa_{\varphi+\varphi_e}(n)^2 \sin 3\eta$ [9, 12]. The band gap and the band-edge effective mass $m^*$ are

$$\varepsilon^K_G(n) \approx 2\gamma \big| \kappa_{\varphi+\varphi_e}(n) \big| \Big( 1 + \frac{\beta a \kappa_{\varphi+\varphi_e}(n)}{4\sqrt{3}} \cos 3\eta \Big), \tag{11}$$

$$\frac{1}{m^*} \approx \frac{\gamma}{\hbar^2 \big| \kappa_{\varphi+\varphi_e}(n) \big|} \Big( 1 - \frac{7\beta a \kappa_{\varphi+\varphi_e}(n)}{4\sqrt{3}} \cos 3\eta \Big). \tag{12}$$

The correction of the effective mass is seven times as large as that of the band gap and they are both largest for $\eta = 0$ (zigzag nanotube). These higher-order effects give dependence of the transition energies on $\eta$, but its exact estimation is not easy because of the strong electron-electron and excitonic interaction.

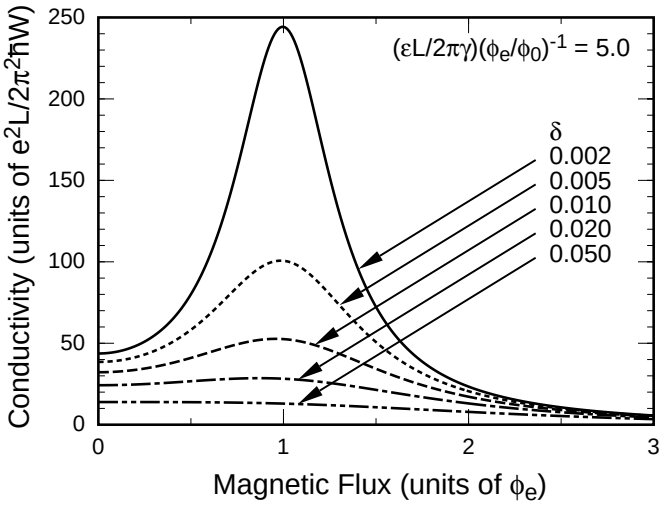


**Figure 4.** Calculated Boltzmann conductivity as a function of AB magnetic flux for a fixed Fermi energy $\varepsilon$. The relative contribution of short-range scatterers is denoted by $\delta$.

## 5. Aharonov-Bohm effect on transport

Metallic nanotubes are known as a ballistic conductor due to the absence of backward scattering as long as the potential range of scatterers is not smaller than the lattice constant of two-dimensional graphite [7, 8]. When several bands are occupied, a perfectly conducting channel transmitting through the system without being scattered back is present [27]. These intriguing features are due to the topological anomaly of the Weyl equation mentioned previously. The presence of both effective flux $\varphi_e$ and AB flux $\phi$ and scatterers with potential range smaller than the lattice constant have a strong influence on this behavior [9].

Figure 4 shows an example of calculated Boltzmann conductivity as a function of AB flux $\phi$ when the band with $n = 0$ is occupied by electrons at the K and K' points [28]. We have assumed the presence of short-range scatterers contributing to the backward scattering even in the absence of flux and scatterers with potential range larger than the lattice constant. The strength of the total scattering is characterized by a dimensionless quantity $W$ and the relative amount of short-range scatterers is denoted by $\delta$. Further, the effective flux due to curvature and strain is denoted by $\varphi_e$. The conductivity exhibits a huge peak at $\varphi = \varphi_e$ where the gap at the K or K' point due to $\varphi_e$ vanishes and only short-range scatterers contribute to the backscattering. The peak conductivity becomes infinite in the absence of short-range scatterers. With the increase of the amount of short-range scatterers the peak becomes smaller and vanishes for sufficiently large $\delta$. Various information on curvature and strain effects and the relative amount of short-range scatterers can be obtained by careful measurement of the conductivity in the presence of the magnetic flux and by changing the electron density through a gate voltage in metallic nanotubes.

## Acknowledgments

The author acknowledges collaboration with H. Ajiki, H. Suzuura, H. Sakai, and T. Nakanishi. This work has been supported in part by a 21st Century COE Program at Tokyo Tech

“Nanometer-Scale Quantum Physics” and by Grant-in-Aid for Scientific Research from the Ministry of Education, Culture, Sports, Science and Technology, Japan.

## References

[1] Ajiki H and Ando T 1993 *J. Phys. Soc. Jpn.* **62** 1255

[2] Ajiki H and Ando T 1993 *J. Phys. Soc. Jpn.* **62** 2470; 1994 *ibid* **63** 4267 (Erratum)

[3] Ajiki H and Ando T, 1994 *Physica B* **201** 349

[4] Wallace P R, 1947 *Phys. Rev.* **71** 622

[5] Slonczewski J C and Weiss P R 1958 *Phys. Rev.* **109** 272

[6] Berry M V 1984 *Proc. Roy. Soc. London* **A392** 45

[7] Ando T, Nakanishi T and Saito R 1998 *J. Phys. Soc. Jpn.* **67** 2857

[8] Ando T and Nakanishi T 1998 *J. Phys. Soc. Jpn.* **67** 1704

[9] Ando T 2005 *J. Phys. Soc. Jpn.* **74** 777 and references cited therin

[10] Ando T 2000 *J. Phys. Soc. Jpn.* **69** 1757

[11] Suzuura H and Ando T 2002 *Phys. Rev. B* **65** 235412

[12] Ando T 2004 *J. Phys. Soc. Jpn.* **73** 3351

[13] Tian W -D and Datta S 1994 *Phys. Rev. B* **49** 5097

[14] Ajiki H and Ando T 1995 *J. Phys. Soc. Jpn.* **64** 4382

[15] Suzuura H and Ando T *Proceedings of 25th International Conference on the Physics of Semiconductors*, edited by Miura N and Ando T (Springer, Berlin, 2001), p 1525

[16] McClure J W 1956 *Phys. Rev.* **104** 666

[17] Ajiki H and Ando T 1994 *Physica B* **201** 349; 1995 *Jpn. J. Appl. Phys. Suppl.* **34-1** 107

[18] Ando T, 1997 *J. Phys. Soc. Jpn.* **66** 1066

[19] Taft E A and Philipp H R 1965 *Phys. Rev.* **138** A197

[20] Sakai H, Suzuura H and Ando T 2003 *J. Phys. Soc. Jpn.* **72** 1698; 2004 *Physica E* **22** 704

[21] Ichida M, Mizuno S, Tani Y, Saito Y and Nakamura A 1999 *J. Phys. Soc. Jpn.* **68** 3131

[22] Ichida M, Mizuno S, Saito Y, Kataura H, Achiba Y and Nakamura A, 2002 *Phys. Rev. B* **65** 241407

[23] Bachilo S M, Strano M S, Kittrell C, Hauge R H, Smalley R E, and Weisman R B 2002 *Science* **298** 2361

[24] Zaric S, Ostojic G N, Kono J, Shaver J, Moore V C, Strano M S, Hauge R H, Smalley R E and Wei X 2004 *Science* **304** 1129

[25] Zaric S, Ostojic G N, Kono J, Shaver J, Moore V C, Hauge R H, Smalley R E and Wei X 2004 *Nano Lett.* **4** 2219

[26] Ajiki H and Ando T 1996 *J. Phys. Soc. Jpn.* **65** 505

[27] Ando T and Suzuura H 2002 *J. Phys. Soc. Jpn.* **71** 2753

[28] Nakanishi T and Ando T J. Phys. Soc. Jpn. (submitted for publication)